Atmos. Chem. Phys., 10, 8629–8647, 2010
www.atmos-chem-phys.net/10/8629/2010/
doi:10.5194/acp-10-8629-2010

Atmospheric Chemistry and Physics

Baseline levels and trends of ground level ozone in Canada and the United States

E. Chan and R. J. Vet

Air Quality Research Division, Science and Technology Branch, Environment Canada, 4905 Dufferin Street, Toronto, Ontario, M3H 5T4, Canada

Received: 24 August 2009 – Published in Atmos. Chem. Phys. Discuss.: 7 October 2009
Revised: 9 September 2010 – Accepted: 10 September 2010 – Published: 16 September 2010

Abstract. A statistical method was developed to extract *baseline* levels of ground level ozone in Canada and the US, and to quantify the temporal changes of *baseline* ozone levels on annual, seasonal, diurnal and decadal scales for the period 1997 to 2006 based on ground-level observations from 97 non-urban monitoring sites. *Baseline* ozone is defined here as ozone measured at a given site in the absence of strong local influences. The quantification of *baseline* levels involved using a Principal Component Analyses (PCA) to derive groups of commonly-varying sites in contiguous regions by season, followed by using backward air parcel trajectories to systematically select ozone mixing ratios associated with the *baseline* condition in each of the PCA-derived regions. Decadal trends were estimated by season for each of the regions using a generalized linear mixed model (GLMM).

Baseline ozone mixing ratios determined by this method were found to vary geographically and seasonally. For the 1997–2006 period, *baseline* mixing ratios were calculated for annual and seasonal periods in seven regions of North America based on multi-site multi-year averages of the *baseline* data sets. The annual average (±1 standard deviation) *baseline* mixing ratios for the regions are as follows: Continental Eastern Canada=30±9 ppb, Continental Eastern US=30±10 ppb, Coastal Eastern Canada=27±9 ppb, Coastal Western Canada=19±10 ppb; Coastal Western US=39±10 ppb, Continental Western Canada=28±10 ppb and Continental Western US=46±7 ppb. Trends in the *baseline* mixing ratios were also found to vary by season and by geographical region. On a decadal scale, increasing *baseline* ozone trends (temperature-adjusted) were observed in all seasons along the Pacific coasts of Canada and the US, although the trends in California were not statistically significant. In the coastal zone of Pacific Canada, positive trends were found with a rate of increase of 0.28±0.26, 0.72±0.55, and 0.93±0.41 ppb/a in spring (MAM), summer (JJA) and winter (DJF), respectively. In the Atlantic coastal region, the trends were also positive in 3 of the 4 seasons (but only significantly so in MAM). In the high ozone precursor emission areas of the Eastern United States, decadal trends in *baseline* ozone are, in general, negative in the spring, summer and fall and appear to be controlled by the strong within-region changes induced by decreasing ozone precursor emissions.

Correspondence to: E. Chan
(elton.chan@ec.gc.ca)

1 Introduction

Tropospheric ozone is an important atmospheric species. It constitutes a major component of photochemical smog and has serious health effects on humans (Burnett et al., 1996) and vegetation (Karlsson et al., 2009). The associated costs of health care and damage to vegetation has been estimated at billions of dollars annually in Canada alone (Canada, 2007). Ozone also regulates atmospheric oxidation potential through the control of hydroxyl radicals (OH) with OH being the dominant *cleansing* chemical in the atmosphere, annually removing gigatons of reactive trace gases including greenhouse gases (GHGs) (Ehhalt, 1999; Prinn, 2003).

The Intergovernmental Panel on Climate Change (IPCC, 2001, 2007) indicates that tropospheric ozone is the third most important anthropogenic GHG, following CO_2 and CH_4. As the global temperature continues to rise, more favourable conditions for ozone formation will occur, e.g., through increased isoprene availability and soil-NO_x emissions (Zeng et al., 2008) and wildfires (Jaffe et al., 2008). Since tropospheric ozone is expected to have a direct positive radiative forcing on climate (Ramaswamy et al., 2001), this possible feedback mechanism may warm the earth's atmosphere further in the future. However, it remains unclear whether tropospheric ozone levels will indeed increase or decrease in a warmer climate since increased water vapor can

shorten the atmospheric lifetime of ozone (Johnson et al., 1999; Gauss et al., 2006; Stevenson et al., 2006; Wild, 2007; The Royal Society, 2008). Modeling studies have shown that there is a strong inter-relationship between tropospheric ozone, CH_4, climate and regional air quality (West et al., 2007; Fiore et al., 2008). Therefore, a comprehensive data analysis and the quantification through observations of different ozone levels and temporal variations within the troposphere are needed in current atmospheric research. It should be noted at this point that ground-level ozone is considered in this study to extend from 0-10 m above ground level while tropospheric ozone is considered to extend from ground level to 10–20 km above ground.

The term *background* is often used in atmospheric science to describe mixing ratios at *clean, remote* sites (Altshuller, 1987; Altshuller and Lefohn, 1996; Lin et al., 2000; Lefohn et al., 2001; Jaffe et al., 2003; Vingarzan, 2004; Oltmans et al., 2008). However, for relatively well-mixed secondary pollutants such as ozone, all sites in the northern hemisphere are influenced in some way and at some time by anthropogenic emissions, which makes the use of this term ambiguous. The term *baseline* is used here to describe ozone mixing ratios in air masses that have not been affected by local anthropogenic precursor emissions. Various methods are used to define, diagnose and estimate *baseline* conditions, but these are not straightforward since measurements at a particular location can include contributions from local anthropogenic and natural precursor emissions, distant natural emissions, and distant anthropogenic emissions. The latter three components, as a function of upwind emission region, are included in the definition of *baseline* in this paper. Since *baseline* ozone is not directly observable, all observation-based research on the topic, including this study, use measurement data to estimate *baseline* levels and how they have been changing. In contrast, the term global or hemispheric *background* is terminology used in modelling that estimates the atmospheric mixing ratio or concentration of a pollutant due to natural sources only (TF HTAP, 2010). The term *background* was used in Fiore et al. (2003) who quantified it for the US using a chemical transport model as the combination of naturally and anthropogenically produced ozone from outside of the US, plus naturally formed ozone within the US. Similarly, the US Environmental Protection Agency (EPA, 2006) uses the term *Policy Relevant Background* (PRB) as those ozone levels that would exist in the absence of North American emissions. Quantifying this type of *background* is clearly impossible using observations due to the fact that North American emissions cannot be completely turned off in order to make direct atmospheric measurements. However, it remains that estimating *baseline* levels is complicated by the fact that this unobserved, derived entity varies substantially depending on meteorology, geographic area, elevation, season, and averaging time (Altshuller and Lefohn, 1996).

Quantitative estimates of *baseline* ozone mixing ratios in the planetary boundary layer (PBL) in the US have been made from observations (Altshuller and Lefohn, 1996; Lin et al., 2000; Lefohn et al., 2001) and global chemical transport models (GEOS-Chem) (Fiore et al., 2003; Wang et al., 2009). Trends in *baseline* ozone have also been published with various papers showing significantly increasing *baseline* ozone in the Northern Hemisphere (Jaffe et al., 2007; Ordóñez et al., 2007; Derwent et al., 2007; Jenkin 2008; Tanimoto 2009; Parrish et al., 2009; Cooper et al., 2010) and other papers showing varying changes, i.e., positive at some locations, not significant at others (Oltmans et al., 2006, 2008). Derwent et al. (2003) used a photochemical trajectory model to describe regional-scale ozone levels and trends using the *worst case* meteorological situation and commented on the potential confounding influence of a changing global ozone *baseline* on determining the impact of domestic precursor emissions. In Chan (2009), a multiple-site ensemble time series modelling technique was applied to characterize a decadal change in the ozone mixing ratios. This was done using different averaging metrics for the period 1997 to 2006 for many regions in Canada and the US. The evidence from that particular study showed significant decreasing trends in southeastern Canada and the eastern US but increasing trends in coastal regions. However, no data screening was done to determine ozone mixing ratios associated solely with the *baseline* air. That is the subject of this paper.

In this study, a new method is introduced whereby *baseline* ozone data are defined by the subset of measured data that corresponds to a *baseline* air trajectory cluster (one of six possible clusters) associated with the lowest May–September 95th percentile of ozone (i.e., the least amount of regional/local photochemically-formed ozone). The robustness of the decadal *baseline* ozone trend analysis in this paper is strengthened by employing an ensemble site approach to the time series modelling (Chan, 2009). The same statistical technique is applied throughout this paper to provide statistical consistency between the trend estimates of the various regions. What is different from Chan (2009) is that the decadal trends for the *baseline* conditions for various regions are estimated for the four seasons separately. This study provides a comprehensive analysis of *baseline* ozone variations in different chemical regimes/regions – for the first time covering Canada and the US to complement work published on the west coast of the US (Jaffe et al., 2007; Oltmans et al., 2008; Parrish et al., 2009).

2 Data sources

The ground level *non-urban* ozone mixing ratio data for the period 1997 to 2006 used in this study were obtained from the Canadian Air and Precipitation Monitoring Network (CAPMoN), http://www.msc-smc.ec.gc.ca/natchem/, the Canadian National Air Pollution Surveillance Network (NAPS), http://www.etc-cte.ec.gc.ca/ and the United States Clean Air Status and Trends Network (CASTNET) of the

US Environmental Protection Agency and the National Park Service (NPS). Data from CASTNET and NPS are available from: http://epa.gov/castnet/. In all, ninety-seven non-urban measurement sites were used in the two countries, spanning latitudes from approximately 29° N to 55° N, and longitudes from 65° W to 123° W. The altitudes of the sites ranged from 2 to 3178 metres above sea level (a.s.l.). Non-urban sites were used to minimize, as much as possible, local influences present in the data. Temperature observations, used to remove temperature effects in decadal *baseline* ozone trends, were obtained from the Canadian Climate Archive for ozone sites located in Canada and from on-site CASTNET temperature observations for sites in the US.

In the CAPMoN network, the sites are located in rural or remote areas and are considered to be regionally representative. In the NAPS network, only the few sites located in rural locations were used, although, in general, they may have been more influenced by pollution from upwind urban areas than the sites in CAPMoN and CASTNET. Similar to CAPMoN, the CASTNET sites are rural in nature. Six-hour averages of hourly ozone mixing ratios at the measurement sites were used for the investigation of seasonal (intra-annual) variations. To avoid the influence of the nocturnal boundary layer and the effects of local precursor emissions, as well as nighttime scavenging and dry deposition, daytime averages (12:00–18:00 local standard time (LST)) were used for studying the decadal *baseline* ozone trends, i.e., during the time when the PBL is fully developed and the air is expected to be well-mixed. Only sites with 75% or more data capture for every season for both ozone and temperature were used.

Three-day air parcel (single-particle) backward trajectories produced by the Canadian Meteorological Centre (CMC) were used to sort/subset the six-hour-average ozone mixing ratios for this analysis. The trajectory calculations were made at the 925 hPa level for sites located below 1000 metres above sea level. For sites >1000 m a.s.l., the calculations were made at 500 m above site elevation. This was done to minimize the influence of surface effects and to ensure that the trajectories were regionally representative. The CMC trajectories (D'Amours and Pagé, 2001) are driven by 3-dimensional analyzed wind fields with 100 km horizontal resolution calculated by the Canadian Meteorological Centre's Global Environmental Multiscale (GEM) model (Côté et al., 2007) for the study period. The trajectory calculations are not based on isentropic or isobaric assumptions. Trajectories were calculated for arrival times at the measurement sites of 00:00, 06:00, 12:00, and 18:00 UTC every day.

3 Statistical methods

A number of statistical methods were used in sequence to establish the *baseline* ozone levels and trends. They are described as follows.

3.1 Seasonal principal component analysis

Principal Component Analysis (PCA) (SAS/STAT, 1990) was done to group the ozone measurement sites and thereby form specific geographic regions for the *baseline* ozone trend analysis that follows. The objective here was to use PCA to maximize the total variance that could be accounted for by as few physically-meaningful regions as possible (Chan, 2009). PCA is a dimensionality reduction technique that makes no attempt to form regions with equal numbers of sites. The regional groupings were formed using a correlation matrix calculated from the six-hour-average ozone mixing ratios from the 97 non-urban CAPMoN, NAPS, CASTNET and NPS sites for the period 1997–2006 during the months of March-April-May (MAM), June-July-August (JJA), September-October-November (SON) and December-January-February (DJF) separately. Similar to Eder et al. (1993), a varimax orthogonal rotation was used in this study. Seventy-five percent was the minimum total variance that had to be accounted for by the number of underlying principal components in each season.

3.2 Backward air parcel trajectory clustering

A k-means clustering technique (Dorling et al., 1992) based on Euclidean distance was used to sort the three-day air parcel backward trajectories from 1997 through 2006 into six trajectory clusters for each site. The method of determining the number of clusters (6) was the same as that used in Dorling et al. (1992). A graph was plotted for the total root mean square deviation (TRMSD) of all individual clusters from their cluster mean vector against the number of clusters retained. A jump in the TRMSD plot (not shown) at seven clusters indicated that six was the optimal number of clusters that should be used. Six clusters were found to be common to most sites and were therefore used throughout this study. In this context, trajectory clusters were considered to characterize the 10-year air flow climatology affecting the measurement sites.

As mentioned above, the trajectory clusters at each site were created from the k-means clustering of the horizontal (i.e., latitude and longitude) displacement of 3-day backward trajectories. One could question why the vertical displacement (i.e., height) of the air parcel trajectories was not used as a third determining factor in the clustering analysis and why three-day trajectories were selected over other periods. The vertical displacement was not included because: (1) horizontal displacement provides a much stronger deterministic factor than vertical displacement since the former varies over hundreds of kilometers while the latter varies over only tens of kilometers (and usually less), (2) the horizontal displacement captures the spatial distribution of the precursor emission sources more so than does the vertical displacement, and (3) the addition of the vertical displacement to the horizontal displacement would create many more trajectory clusters

which means that the *baseline* clusters and their mixing levels would be difficult to define. Three-day back trajectories were chosen because they typically extend beyond the PCA-derived regions and they represent the typical period between frontal passages, which are responsible for major wind direction changes and for restarting the accumulation of ozone in the boundary layer.

After every three-day trajectory at a site was assigned to one of six trajectory clusters, its associated six-hour average ozone mixing ratio was then assigned to its appropriate trajectory cluster and the 95th percentile ozone mixing ratio for May to September was calculated for each cluster. The *baseline* trajectory cluster was chosen for each site as the one having the lowest 95th percentile ozone mixing ratio of the six clusters. This cluster was assumed to represent *baseline* air flow with the least influence of regional and local-scale photochemically-produced ozone (which generally contribute to peak levels in the summer). The 95th percentile value was chosen because, for remote locations, it is thought to be predominately associated with long-range transport, while lower percentile values (such as the median or 75th percentile) are affected by dry deposition and NO scavenging which serve to reduce the ozone mixing ratios. To provide contrast and context to the *baseline* results, the trajectory cluster associated with the highest 95th percentile at each site was selected and identified as the *most polluted* data set. The *most polluted* data and the associated air masses can be viewed as an analogy to the *worst case* meteorology (Derwent et al., 2003).

3.3 Seasonal and diurnal cycles

LOcally WEighted Scatter plot Smoothing (LOWESS) (Cleveland et al., 1988; SAS/STAT, 1990) was used to display the seasonal and diurnal cycles at each site in each PCA-derived region using the JJA groupings. The smoothing parameter was chosen such that the periodicities of the temporal variations were between a month and a year for the seasonal cycles, and less than 24 hours for the diurnal cycles.

3.4 Regional decadal *baseline* ozone trends for different seasons

A generalized linear mixed model (GLMM) (SAS/STAT, 2006), which serves as a multiple site ensemble technique, was used to discern a decadal ozone trend for each PCA-derived region as a whole. The multiple site approach was used to increase the amount of data and thereby increase the robustness of the decadal *baseline* ozone trend estimates. No interpolation was done to fill the missing data gaps as this was not necessary using GLMM (Littell et al., 2006), which is one of the important advantages of GLMM. The details of the time series model have been previously described in Chan (2009); here, however, the model was run for each season separately.

In this time series model, the effects of inter- and intra-annual variations due to warmer versus colder weather were accounted for by using the daily maximum 1-hr temperature as the covariate. The model also contained a one-day autoregressive term. The physical meaning behind the choice of one-day autoregression is that it represents the short-term day-to-day temporal correlations due to very similar meteorological conditions from one day to the next. Sine and cosine terms with three- to five-year periodicities were used to model the decadal trend component instead of a polynomial, which is often used. This was done to avoid collinearity with the linear slope term with respect to time. Neither one-year nor six-month harmonic terms were included because the regional trend analyses were done for different seasons separately.

3.5 Baseline ozone mixing ratio levels and seasonal and diurnal variations

The method developed in this study uses the knowledge of ozone temporal behavior in response to regional photochemistry in combination with trajectory clustering to objectively select the *baseline* and *most polluted* clusters for each site. Again, the *most-polluted* clusters are included here as a basis for contrasting the results of the *baseline* clusters. Seasonal *baseline* ozone levels and temporal variations were calculated by fitting a one-year harmonic cycle to all six-hour-average data associated with the *baseline* clusters for seven regions, namely: 1) Coastal Eastern Canada, 2) Continental Eastern Canada, 3) Coastal Western Canada, 4) Continental Western Canada, 5) Continental Western US, 6) Continental Eastern US and 7) Coastal Western US/Interior California. Similarly, the diurnal *baseline* ozone levels and variations were estimated by fitting a 24-h cycle to all the hourly data associated with the *baseline* air clusters for the different seasons for the seven regions.

4 Results and discussion

4.1 Seasonal principal component analysis

The varimax orthogonal rotation identified 13, 14, 11, and 8 individual PCA-derived regions for the MAM, JJA, SON, and DJF seasons, respectively. The PCA-derived regions (or principal components) were ordered by the percentage of the total variance explained from the largest to the smallest. Sites that were grouped together had the largest PCA loadings associated with that particular region (principal component). Figure 1 shows, for the four seasons, the different PCA-derived regions of measurement sites with the same symbols. In general, from season to season the same regions exist with the exception of winter, for which there were fewer regions (indicating more spatial homogeneity than the other seasons). Figure 2 shows, for each season, the 10-year-average three-day backward trajectory at each site. It can be

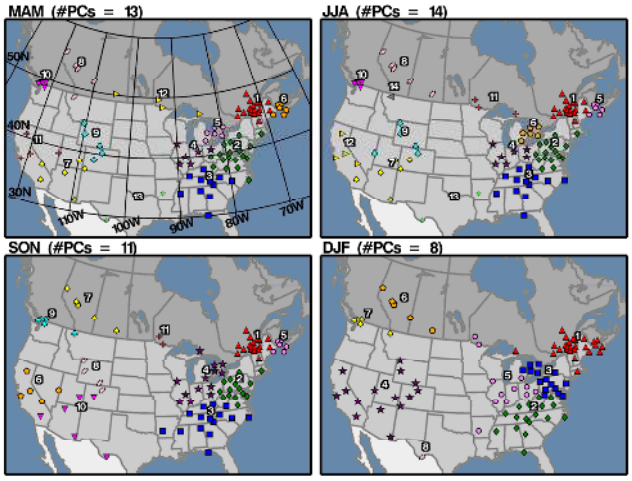

Fig. 1. Results of rotated PCA analysis using six-hour ozone mixing ratio averages for the period 1997–2006 for different seasons. The number of regions in the season is shown in the bracket on top of each panel. The seasonal breakdowns are as follows: spring (MAM), summer (JJA), fall (SON), and winter (DJF). Sites that have the same symbols belong to the same region for a given season. See text for more details.

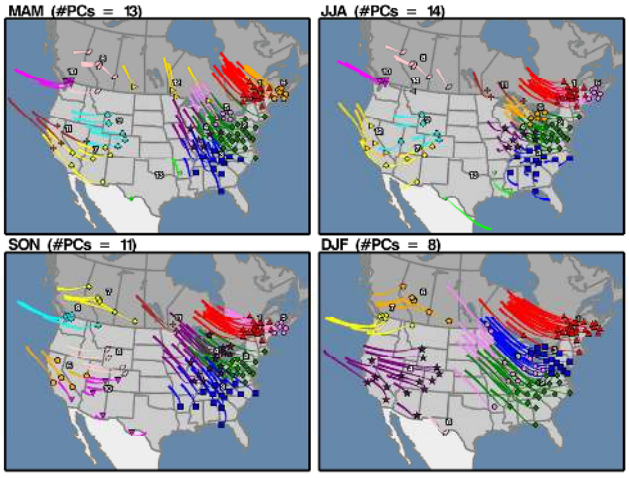

Fig. 2. Average three-day backward air parcel trajectories for each ozone measurement site for the period 1997–2006 for different seasons.

seen that these average trajectories (averaged from all trajectories, not just the *baseline* trajectories) at all sites within a given region have similar average flow directions. This implies that the precursor emission sources in the upwind direction are, on average, similar for most sites in each region.

4.2 Backward air parcel trajectory clustering

One site, Egbert (44° 13′57″ N, 79° 46′53″ W), Ontario, Canada, was selected to illustrate the use of trajectory clustering to classify the ozone mixing ratio data. First, six trajectory clusters were established (Fig. 3a) for this and every site. Then, each six-hour average ozone mixing ratio was assigned to its associated trajectory and binned into its appropriate trajectory cluster. In Fig. 3a, the cluster number (C1 to C6) is shown at the top left of each cluster panel and the relative transport frequencies (in percentages for different seasons), are shown at the bottom left corner. For example, C1 represents the cluster of southwesterly flow trajectories and contains a total of 2471 (17%) trajectories throughout the period 1997–2006. Comparing across the six clusters for the same season, the transport frequencies attributed to this cluster are 15%, 17%, 20%, and 16% during spring (MAM), summer (JJA), fall (SON), and winter (DJF), respectively. Figure 3b shows a monthly box-and-whisker plot of the six-hour-average ozone mixing ratios (ppb) associated with the six clusters. The May–September 95th percentiles for the southwesterly flow (C1) and northerly flow (C6) are shown as the red and yellow horizontal bars, respectively. In this case, C6 was selected as the *baseline* cluster for this site because its May–September 95th percentile mixing ratio was the lowest (yellow bar) of the six clusters. The choice of C6 as the *baseline* cluster is further validated by the fact that: (1) a summer maximum, which is typically attributed to within-region or local photochemically-produced ozone, does not exist. and (2) the 5th percentile (lower whisker) value is the highest of the six clusters in the winter, suggesting that it is representative of *baseline* conditions because the ozone mixing ratios do not show evidence of the destruction (i.e., NO titration) typical of clusters influenced by western and southern NO_x emission areas.

Monthly 95% multiple Bonferroni test results are shown at the top of Fig. 3b; the Bonferroni test is a conservative test used to control family-wise testing error. The clusters are ordered from highest (top) to lowest (bottom) based on the magnitude of the monthly mean mixing ratios associated each cluster. Vertical bars that overlap the different clusters indicate that there is no evidence of significant statistical differences between those clusters; alternatively, clusters not joined by vertical bars are considered to be significantly different. For example, the *baseline* cluster, C6, which represents predominantly northerly flow, has the lowest monthly mean ozone mixing ratios during the summer months of JJA but is not significantly different from the C4 mean in most of the other months except October and November, where C4 is a shorter transport cluster that has more northerly and easterly components than C6. The Bonferroni testing therefore clarifies that the *baseline* mixing ratios are not significantly different from the C4 mixing ratios in most months of the year, thereby giving further credibility to the fact that predominantly north and northwesterly flow is little influenced by within-region and local precursor emissions. In contrast, the *most polluted* cluster, C1, is often associated with the highest monthly mean ozone mixing ratios during

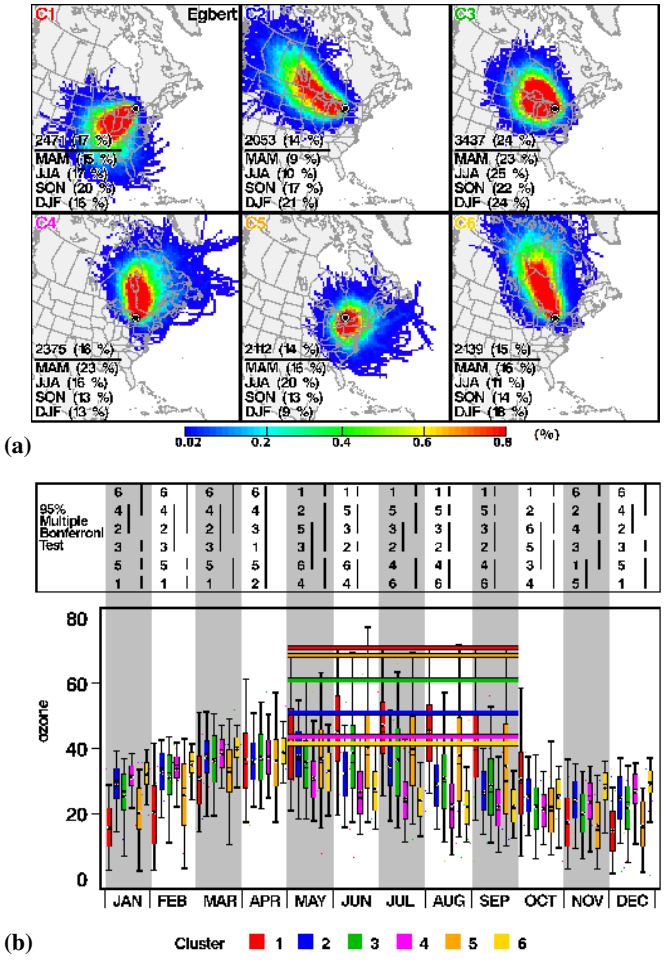

Fig. 3. **(a)**: Probability density plots of backward trajectories for Egbert (44° 13′57″ N, 79° 46′53″ W), located in Ontario, Canada. Trajectory clusters are shown as probability density plots whereby the blue-to-red colors in the grid squares represent the relative frequency with which trajectories passed over the grid squares (calculated as the number of trajectories in the cluster passing over a grid square divided by the total number of trajectories passing over all grid squares in all clusters). Shown only are the grid cells with probability greater than 0.02. Those grid cells with probability greater than or equal to 0.8 are shown with the same color. **(b)**: Monthly box-and-whisker plot of the six-hour-average ozone mixing ratios (ppb) associated with the trajectory clusters in Fig. 3a. The endpoint of the upper whisker, upper edge, dot inside, line inside, lower edge of the box and endpoint of the lower whisker show the 95th, 75th, mean, median, 25th and 5th percentiles, respectively.

May through October and the means are always significantly different from the other clusters in the warm months.

Figure 4a and b show the *baseline* and *most polluted* air parcel trajectory clusters for the most statistically representative site in each cluster/region, i.e., the site with the largest communality value associated with the respective principal component for the JJA months. Note that the larger the communality of a site in the principal component, the better the site is explained by the respective principal component and thus, the more representative it is of the region. In Fig. 4b, the trajectory clusters shown are the ones associated with the highest May–September 95th percentile ozone mixing ratios of the six clusters at each site. These clusters represent the *most polluted* air flows affecting the sites and have been included to provide a contrast to the *baseline* air flows shown in Fig. 4a. It is important to emphasize here that the statistics used to select the *baseline* trajectory clusters were based on May to September ozone data while the trajectory clusters themselves were produced from data from all months in the 1997 to 2006 time period.

Generally, *baseline* air clusters (Fig. 4a) at non-coastal sites are associated with trajectories originating in high altitude (altitude statistics not shown) over adjacent low precursor emission areas, whereas for coastal sites, they are associated with oceanic (Pacific or Atlantic) flows. For the most part, the *baseline* air trajectory clusters traverse areas with minimal regional anthropogenic precursor sources (see the population density map shown in the centre of Fig. 4a). Although less important for the non-urban sites, it is important to note that the *baseline* value estimated may still be affected by ozone removal processes such as NO scavenging. In addition, dry deposition by vegetation may play an important role at non-urban sites. The methods used in this paper have made no attempt to remove the effects caused by these two processes. However, the existence of such removal processes was evaluated by selecting the *most polluted* air clusters as discussed later in this section. The transport frequency statistics of the *baseline* air clusters are shown in the lower left corner of the trajectory probability density panels. The statistics show that the *baseline* clusters tend to have the highest frequency of annual trajectories in the winter (DJF) and spring (MAM) months when *baseline* air is typically being transported at higher altitude and over longer distance in the northern mid-latitudes (Wang et al., 2003).

Figure 4b presents the *most polluted* clusters for the same 14 representative sites, one in each region. In this *most polluted* set of clusters, the transport distance is shorter and closer to the surface (not shown). With the exception of the regions characterized by mountainous terrain, the average transport height of the *baseline* set of clusters is consistently about one km higher than the *most polluted* set of clusters. As well, the transport frequency statistics of the *most polluted* clusters at most sites show the opposite temporal character to the *baseline* air clusters in that the *most polluted* clusters have relatively more frequent air flows during the summer (JJA) and fall (SON) months when photochemistry is at its maximum.

4.3 Seasonal variations of *baseline* mixing ratios

Many studies in the past have discussed the seasonal variations of ground level ozone. Typical for ozone in the Northern Hemisphere is a springtime maximum (Simmonds et al.,

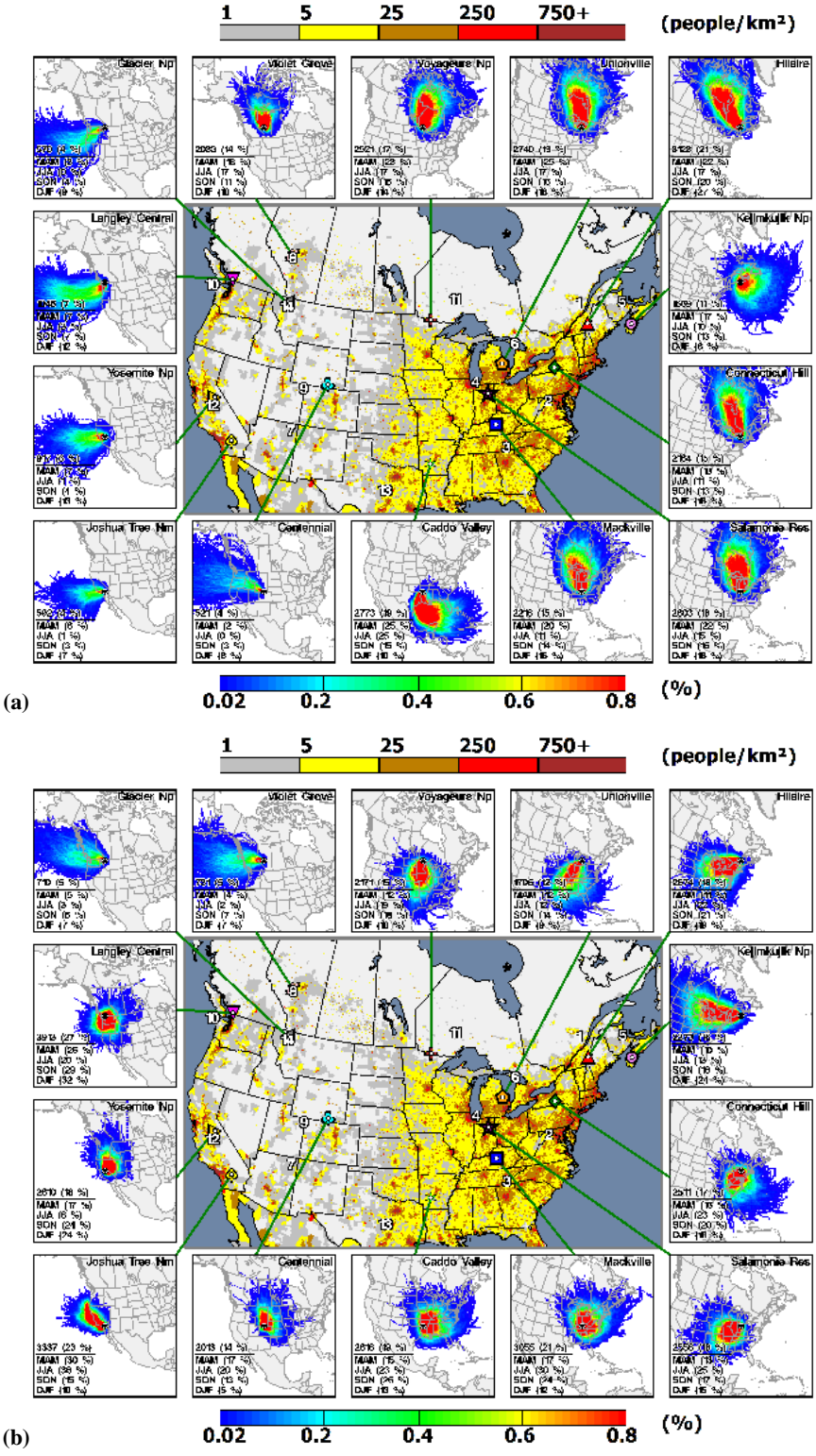

Fig. 4. **(a)** Probability densities of air parcel trajectory clusters (*baseline* air) associated with the lowest May–September 95th percentile ozone mixing ratios for 14 statistically representative sites (out of 97 in total) for the years 1997–2006 combined. The total number of trajectories for the cluster and the transport frequency (in bracket, %) is shown above the horizontal bar. The relative seasonal transport frequencies (relative to other five clusters) are shown below the bar (other five clusters not shown). Population data were taken from CIESIN (2005). **(b)** Probability densities of air parcel trajectory clusters (*most polluted* air) associated with the highest May–September 95th percentile ozone mixing ratios for 14 statistically representative sites (out of 97 in total) for the years 1997–2006.

1997; Monks, 2000), formed partly from enhanced photochemistry in the springtime after a wintertime accumulation of air pollutants (Penkett and Brice, 1986) and partly from a downward flux of stratospheric ozone (Daniesen and Mohnen, 1977; Viezee et al., 1983). A second major temporal characteristic is a summertime maximum that occurs in regions strongly affected by the photochemical production of ozone due to precursor emissions (Singh et al., 1978; Logan, 1985).

To investigate whether these characteristics occur at the sites in this study, the seasonal variations of ozone associated with the *baseline* and the *most polluted* clusters for all sites are shown in Fig. 5a and b. The JJA set of site groupings was used because it had the most regions and thereby revealed the spatial homogeneity of the *baseline* ozone seasonality. With reference to the *baseline* air clusters in Fig. 5a., the high springtime ozone peak and the absence of high summertime values in all regions except PC2, PC3 and PC4 suggest the lack of strong local/regional photochemical ozone production (Goldstein et al., 2004), and also suggests the strong influence of long-range transport to the site with air descending either from the Pacific, Arctic or Atlantic Oceans and, in some cases, northern continental Canada (as shown earlier). In contrast, the influence of within-region, precursor-induced photochemistry in the US appears to be strong in regions PC2, PC3 and PC4 (eastern, southeastern and Midwest US regions) because of the presence of high summertime values. Not surprisingly, this suggests that even for these non-urban sites, the *baseline* mixing ratios are affected by within-region and/or local photochemistry for those regions located very close to high density precursor sources and/or where the frequency of subsidence inversions is high (Fiore et al., 2002, 2003). In addition, because of the similarity of the within-region seasonal profiles and the narrow range of between-site variability over such large spatial scales, the method developed here provides confidence that the selection of the *baseline* air is consistent with the minimal existence of any regional-scale photochemical influence in the less populated and less industrialized regions. It should be noted that in some areas, although the regional-scale influence is small or non-existent, the influence of surface deposition is likely present in each trajectory cluster at each site. In Fig. 5a, the difference in ozone mixing ratios between different regions clearly demonstrates that no uniform *baseline* exists, and the unavoidable influence of surface deposition clearly implies that the measured ozone at any surface site cannot represent a totally unperturbed *baseline* without careful selection to avoid depositional effects. It should be pointed out that this paper does not attempt to separately analyze the possible effects of ozone accumulation due to subsidence or to remove any depositional effects.

In contrast to the foregoing, the seasonal variations associated with the *most polluted* air trajectory clusters (Fig. 5b) show that most of the measurement sites are affected by the higher than-baseline spring maximum and the broad higher summer maximum, both of which are typically associated with the photochemical oxidation of ozone precursors in areas associated with high precursor emission sources. The relatively wide range of the inter-percentile bars (the monthly 5th to 95th percentiles of all sites within the PCA-derived region) shown in Fig. 5b, compared to Fig. 5a, indicates that more within-region and/or local processes have affected the ozone mixing ratios.

At many of the western sites, there is little statistical difference in the seasonal cycles of the trajectory clusters. In these cases, one might consider that more than one trajectory cluster at a given site is representative of *baseline* ozone levels. However, deciding which of the trajectory clusters would be reasonably representative of baseline levels at each site for each month would be difficult and confounding. One potential method would be to carry out a Bonferonni analysis at every site for every month to determine which of the clusters were not significantly different from each other (see Fig. 3b for the Bonferonni results at the Egbert, Canada site). Following this, the *baseline* ozone data from the non-differing clusters could be combined into a single *baseline* data set for each multiple-site region. While this could have been done, it was not because it was felt that the results would have been too confounding to understand and explain, e.g., every PCA-derived region would have had *baseline* levels, cycles and trends derived from different trajectory clusters selected for each month at each site. Instead, the method chosen here provides a clear, practical and well defined concept of *baseline* ozone and its levels, cycles and trends. The foregoing situation at western sites does not apply to sites in the Eastern Continental US (i.e., PC2, PC3 and PC4) where the seasonal cycles and levels differ for the different trajectory clusters and, in doing so, clearly reflect the influence of strong and/or numerous local and within-region precursor sources. Thus, with the exception of these 3 regions, the *baseline* ozone levels in Canada and the US for the most part are indicative of extra-regional precursor source influences, both natural and anthropogenic.

.

4.4 Baseline ozone levels (annual and seasonal)

Annual and seasonal average (± 1 standard deviation) *baseline* ozone levels are tabulated in Table 1 and shown as seasonal cycles in Fig. 6 for each of the following PCA-derived regions: Coastal Eastern Canada (PC5), Continental Eastern Canada (PC1, PC6, PC11), Coastal Western Canada (PC10), Continental Western Canada (PC8), Continental Western US (PC7, PC9), Continental Eastern US (PC2, PC3, PC4) and Coastal Western US/Interior California (PC12). Note that PC12 consists of four sites located in the interior of California and not on the coastline. The calculations of the values shown in Table 1 were done as follows:

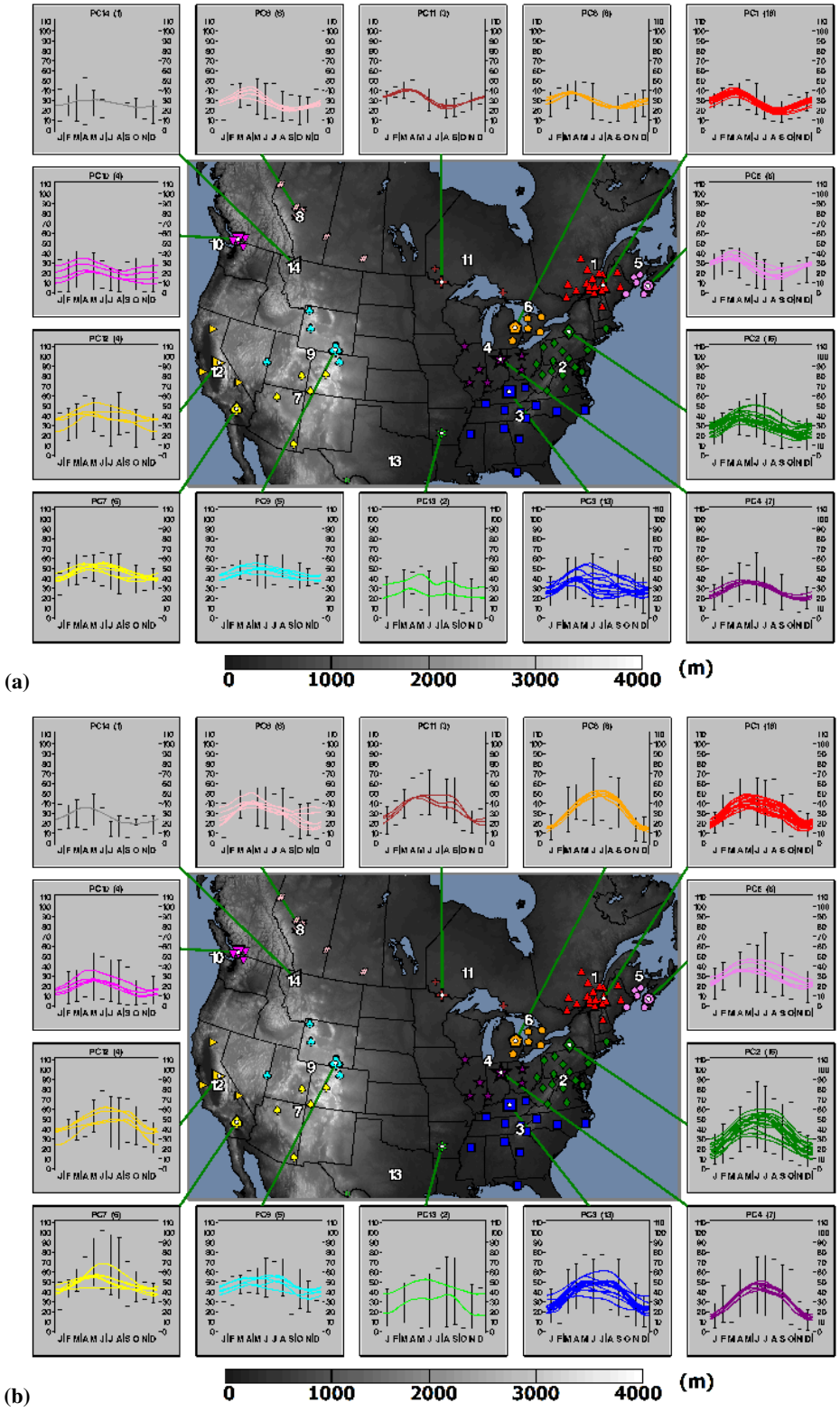

Fig. 5. **(a)**: Seasonal ozone variations generated by LOWESS (see text) associated with the *baseline* air trajectory clusters for all 97 sites. The error bars show the monthly ensemble site 5th to 95th percentiles for the region. The regional groupings are based on rotated PCA for JJA months. Elevations (above sea level, metres) are shown in gray scale from dark to light to represent low to high elevations. Elevations have been normalized to have a minimum of zero metre. **(b)**: Seasonal ozone variations associated with the *most polluted* air trajectory clusters for all 97 sites. Vertical axes represent ozone mixing ratios (ppb) and the tickmarks on the horizontal axes represent the start of each month.

Table 1. Summary of annual and seasonal average (±1 standard deviation) *baseline* ozone mixing ratios (ppb) for seven geographical regions, i.e. Coastal/Continental Eastern Canada, Continental Eastern US, Coastal/Continental Western Canada, and Coastal/Continental Western US. Symbols correspond to Fig. 1: PC1 (red triangles), PC2 (green diamonds), PC3 (blue squares), PC4 (purple stars), PC5 (pink circles), PC6 (orange hexagons), PC7 (yellow spades), PC8 (pink #), PC9 (cyan clubs), PC10 (magenta inverse triangles), PC11 (brown pluses), and PC12 (yellow triangles).

Region	Annual	Seasonal Ranges			
		MAM	JJA	SON	DJF
Eastern Canada (east of 98° W)					
– coastal (PC5)	27±9	34±7	21±8	21±7	31±6
– continental (PC1, PC6 and PC11)	30±9	37±7	24±8	24±7	32±5
Eastern US (east of 98° W)					
– continental (PC2, PC3, and PC4)	30±10	37±9	32±12	25±9	27±7
Western Canada (west of 98° W)					
– coastal (PC10)	19±10	25±11	17±9	15±8	18±9
– continental (PC8)	28±10	36±8	25±10	21±7	29±6
Western US (west of 98° W)					
– coastal (PC12)	39±10	44±10	39±12	38±9	35±8
– continental (PC7 and PC9)	46±7	51±6	48±8	41±5	43±4

– For each of the 7 geographical regions, the *baseline* 6-h average values from all sites were combined into a multiple site, 10-year *baseline* data set (illustrated by the green dots in Fig. 6);

– a *baseline* ozone seasonal curve was calculated for each region by using a least-squared fit with a one-year cycle (red curve in Fig. 6). The resultant seasonal curves shown in Fig. 6 allowed the seasonal patterns of the different regions to be compared;

– the 10-year annual and seasonal average *baseline* mixing ratios (±1 standard deviation) were calculated from the *baseline* data sets in each geographical region (Table 1).

Based on Table 1, the 10-year annual average (±1 standard deviation) *baseline* ozone mixing ratio in Continental Eastern Canada for 1997–2006 was 30±9 ppb and the seasonal average values ranged from a high of 37±7 ppb in the springtime to a low of 24±7 ppb in the fall. Similar levels were found in the Continental Eastern US, where the annual average was 30±10 ppb and the seasonal averages varied from a high of 37±9 in the spring to a low of 25±9 ppb in the fall, as well as in Continental Western Canada, with an annual average of 28±10 and seasonal highs and lows of 36±8 in spring and 21±7 in the fall. In comparison, Coastal Western Canada had the lowest annual and seasonal averages of all 7 geographical areas with values of 19±10, 25±11 and 15±8, respectively.

It is useful to point out that the *baseline* averages mentioned above for Coastal Western Canada are considerably lower than the *inflow Marine Boundary Layer* (MBL) averages (38.6±1.3 ppb for MAM and 30.9±1.0 ppb for SON) reported by Parrish et al. (2009) for the year 2000 (intercept of the linear fit using hourly data from 1991 to 2005) at a site in Olympic National Park site in the same area. There are two major reasons for these differences:

– *different air mass types*: by definition, the values presented in the two studies represent two different types of air, i.e., the Parrish et al. (2009) data represent *inflow* marine boundary layer air from the Pacific Ocean while our results represent synoptic-scale southwest flow, seldom in the marine boundary layer, coupled with long overland transport paths (for 3 of the 4 sites in the region);

– *different sites*: the four sites of Coastal Western Canada differ from the Olympic National Park site used by Parrish et al. (2009) in that they are affected by complex meteorological, orographic, transport and emission influences in the region. As such, the Coastal Western Canada region is strongly influenced by complex land-sea meteorology in the Straits of Georgia and Juan de Fuca (Brook et al., 2004; McLaren et al., 2010), flow-altering orographic and wake effects of Vancouver island and the Coastal Mountains, (Brook et al., 2004) and the occasional accumulation, transport and processing of precursor emissions (leading to the titration of ozone by NO) from the Greater Vancouver Area, the west coast of Washington State, and nearby ship traffic (Hayden et al., 2004; Brook et al., 2004; McLaren et al., 2010).

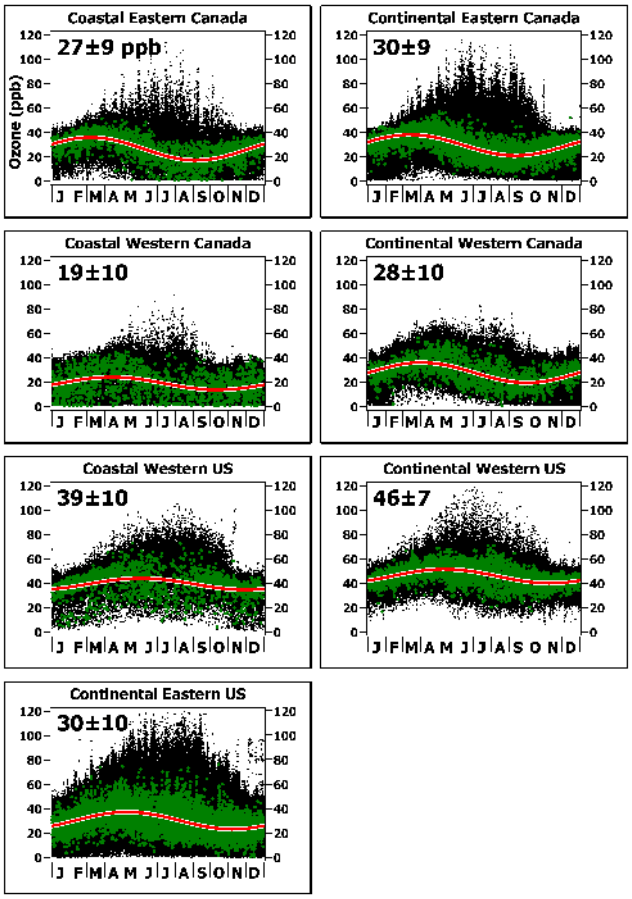

Fig. 6. The seasonal variations of the *baseline* ozone mixing ratios (ppb) relative to all data for Coastal/Continental Eastern Canada, Coastal/Continental Western Canada, Coastal/Continental Western US, and Continental Eastern US regions. The black dots show all of the six-hour averaged mixing ratios for all data from 1997–2006. The green dots show the six-hour averaged mixing ratios associated with the *baseline* air flows. The red fitted curves are the calculated seasonal cycles. The multi-site annual mean (ppb) and ±1 standard deviation are shown in the top left corner for each region

In light of these factors, the abovementioned differences in the *baseline* averages reported herein and in Parrish et al. (2009) are not unexpected and strongly emphasize the importance of carefully defining and understanding the meaning of the term *baseline* in this study.

The Coastal Western US and Continental Western US regions had considerably higher *baseline* levels than the other regions, with annual averages of 39±10 ppb and 46±7 ppb, respectively. In Parrish et al. (2009), during the spring 2002 period of the ITCT 2K2 study at Trinidad Head, a marine boundary layer (MBL) site on the northern California coast, the average results of three tracer criteria used in their study designed to isolate marine air yielded average marine ozone mixing ratios of 42.0 ppb with a standard deviation of 4.4 ppb. This value falls within the range estimated in this 10-year multiple-site study for the Coastal Western US region with 44±10 ppb during the spring (MAM). The high values of the Coastal Western US *baseline* averages compared to those of Coastal Western Canada (elevations ranging from 81 to 178 m a.s.l.) are likely due to the relatively high elevations of two of the sites, i.e., Lassen Volcanic NP (1756 m a.s.l.) and Yosemite NP (1605 m a.s.l.). The high averages (and small standard deviations) of the Continental Western US (annual=46±7, spring=51±6, fall=41±5) are likely due to the high elevation of the sites, thereby sampling the free troposphere with potentially substantial stratospheric ozone inputs.

In general, the seasonal *baseline* averages in Eastern and Western Canada are lower than those in the Western US during the photochemically-active seasons of spring (MAM), summer (JJA) and fall (SON). As well, in the coastal regions of both countries, the *baseline* values are generally lower than in the continental regions, regardless of the season. For JJA, the Canadian regions: PC1 (southern Quebec/northeastern US), PC5 (northern Atlantic Canada), PC6 (southern Ontario), PC8 (Prairie Provinces), PC10 (northern Pacific) and PC11 (western Ontario), have similar seasonal levels and ranges with no presence of the summer maximum that is typically associated with regional photochemically-produced ozone.

Figure 6 illustrates, in addition to the aforementioned seasonal cycle of *baseline* data (red curve), the seasonal variability of the 6-h *baseline* mixing ratios (green dots) relative to the full set of data (black dots) for the six geographical regions. It is apparent from the plots that the *baseline* 6-h values varied considerably when combined over multiple sites and multiple years, but less so than the full data set. These plots show the distribution of the *baseline* data relative to the overall data set for each region. Of particular note is the fact that the *baseline* data set, in spite of representing air that traveled over relatively low anthropogenic precursor emission areas, is quite variable and ranged from <5 ppb to as much as 70 ppb in the Coastal and Continental Western US regions in the spring and summer seasons. This emphasizes the point that *baseline* levels are highly variable because they are affected by inflow of ozone, tropospheric production and/or stratospheric ozone downward mixing (Daniesen and Mohnen, 1977; Viezee et al., 1983; Hocking et al., 2007) to a region plus within-region effects including ozone production from precursor emissions.

4.5 Baseline ozone trends

The decadal (1997–2006) *baseline* ozone trends of daytime (12:00–18:00 LST) average ozone mixing ratios were estimated using the GLMM technique for the four seasons and for all PCA-derived regions. The results are tabulated in Table 2 for trends that are statistically significant at the $p<0.05$ level and for all trend results shown graphically in Fig. 7a and b (for the *baseline* air and *most polluted* air, respectively).

Table 2. Decadal *baseline* ozone trends modelled by GLMM using daytime (12:00 – 18:00 LST) average ozone mixing ratios from 1997 to 2006 by season. Only regions with significant trends (p-value less than 0.05) are shown. *p-values are shown for temperature-adjusted trends only. The trend results are tabulated in ppb per annum. Note that the PC numbers shown in the first column correspond to Fig. 7a and change from season to season. "ABS" stands for the absolute value of the trend.

PC	Season	*p*-value*	Temp-adjusted Trend (ppb/a)	Non-adjusted Trend (ppb/a)	ABS (Temp-adjusted trend) minus ABS (Non-adjusted trend) (ppb/a)
1		0.0002	−0.18±0.1	−0.15±0.1	0.03
2		< .0001	−0.59±0.14	−0.61±0.14	−0.02
3		0.0003	−0.66±0.27	−0.63±0.22	0.03
5		< .0001	−0.21±0.05	−0.18±0.05	0.03
6	MAM	0.0459	0.34±0.34	0.32±0.34	0.02
7		0.008	−0.61±0.45	−0.03±0.47	0.58
10		0.0391	0.28±0.26	0.29±0.3	−0.01
12		0.0215	−0.5±0.39	−0.59±0.33	−0.09
1	JJA	0.0005	0.27±0.15	0.37±0.18	−0.1
2		< .0001	−0.97±0.22	−1.08±0.23	−0.11
3		< .0001	−1.56±0.45	−1.81±0.42	−0.25
4		< .0001	−0.89±0.24	−0.91±0.19	−0.02
8		0.0196	0.38±0.3	0.64±0.24	−0.26
9		0.0119	0.55±0.43	0.58±0.44	−0.03
10		0.0136	0.72±0.55	0.82±1.98	−0.1
1	SON	0.0228	−0.12±0.1	−0.12±0.1	0
2		< .0001	−0.45±0.16	−0.39±0.22	0.06
3		< .0001	−0.74±0.29	−0.91±0.3	−0.17
8		0.0079	−0.39±0.29	−0.61±0.31	−0.22
5	DJF	0.0006	0.7±0.39	0.58±0.38	0.12
6		0.0361	0.66±0.61	1.01±0.62	−0.35
7		<.0001	0.93±0.41	0.88±0.41	0.05

Table 3. A comparison of the statistical methods used and the *baseline* ozone trend estimates focusing on Western Canada and the Western US from three recent papers and this paper.

Authors	Period	Location	Average Metrics	Data Screening Method	Statistical Method	Season	Trend estimate (ppb/a)
Oltmans et al. (2008)	1988–2007, 1999–2007	Western US	Daytime averages	Backward trajectory	Autoregressive model – a cubic polynomial for trend	Winter Spring Summer Fall	Positive at some sites, no significant changes at others.
Jaffe et al. (2007)	1987–2004	Western US (Rocky Mt., Yellowstone, Lasseon)	Daytime monthly means	N/A	Linear regression	Winter Spring Summer Fall	+0.21 to +0.62 +0.33 to +0.59 +0.43 to +0.50 +0.28 to +0.56
Parrish et al. (2009)	Various lengths covering (1974-2007)	West coast of the US	Monthly means	Local wind data	Linear regression	Winter Spring Summer Fall	+0.43±0.17 +0.46±0.13 +0.24±0.16 +0.12±0.14
This paper	1997-2006	Western Canada and the US	Daytime averages	Backward trajectory	Regional trend analysis using GLMM – long-term sinusoidal cycles (3 to 5 years) for trend	DJF (PC7) MAM (PC10) JJA (PC10) SON (PC9)	+0.93±0.41 +0.28±0.26 +0.72±0.55 No significant changes

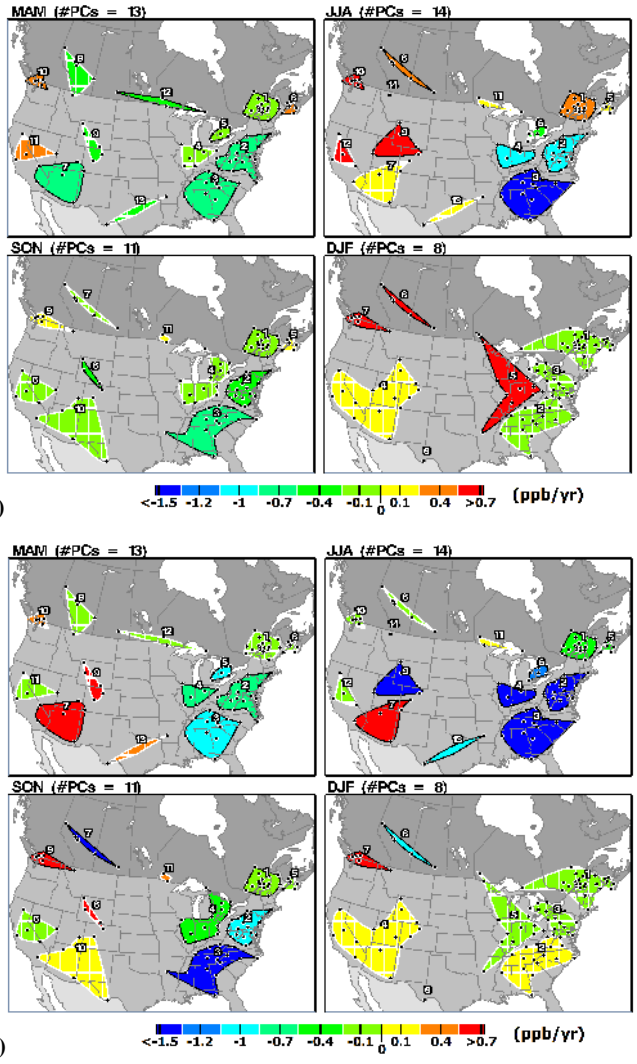

Fig. 7. **(a)**: Regional decadal trends of daytime (12:00–18:00 LST) average ozone mixing ratios associated with the *baseline* air, modelled by GLMM for different seasons. Regions have been previously defined by rotated PCA for different seasons. Significant trends at the 0.05 level are shown with a black regional boundary. The boundaries were determined by joining the outermost site locations from each region. No evidence of statistical significance is shown with a white boundary. The *baseline* air is defined as the air parcel trajectories associated with the lowest May–September 95th percentile ozone mixing ratios at a given site. **(b)**: Regional decadal trends of daytime (12:00–18:00 LST) average ozone mixing ratios associated with the *most polluted* air, modelled by GLMM for different seasons. The *most polluted* air is defined as the air parcel trajectories associated with the highest May–September 95th percentile ozone mixing ratios at a given site.

For comparison purposes, Table 3 provides a summary of *baseline* ozone trends from three recently published papers on ozone trends of inflow air at sites in the Pacific coastal areas of North America (Jaffe et al., 2007; Oltmans et al., 2008; Parrish et al., 2009). Since these three studies used single site trend analyses, it is worth pointing out that the multi-site modelling used herein allows conclusions to be drawn on a regional basis using larger data sets. The authors of the aforementioned three papers report increasing trends, which are in general agreement with this paper although the magnitude of the multi-site trend in that area was greater using the multi-site approach than in the three single site studies. However, the time periods and sites selected were different in these 4 studies, making a direct quantitative comparison impossible.

It is important to note here that the direction of the decadal *baseline* ozone trends in Table 2 is more robust than the magnitude of the trends. This is because the estimated magnitude depends on many factors including: (1) the statistical method chosen, (2) the model formulation, (3) the representativeness and power of the rather small number of data in the *baseline* trajectory clusters (i.e., comprising only 4 to 25% of the total data set from Fig. 5a), (4) the data period, and (5) the fact that the magnitude of the decadal trend is generally much smaller (less than one ppb per year) than the other shorter time-scale trends in the data (tens of ppb from day to day). In light of the relatively small amounts of data associated with the *baseline* clusters, the multiple-site GLMM technique has the advantage compared to other techniques of higher levels of robustness and statistical power from the larger data set. The GLMM time series model and statistical details can be found in Chan (2009).

As mentioned earlier, temperature effects were accounted for in the results shown in Table 2 and Fig. 7 by using daily 1-hr maximum observations as the covariate in the time series model. In some regions, the temperature adjustment resulted in a reversal of trend directions but neither the unadjusted nor adjusted trends were statistically significant in those cases. In general, the temperature adjustment tended to reduce the magnitude of the summer (JJA) trends only, with no systematic reduction or increase in the other seasons. This suggests that the temperature trend varied in the same direction as the ozone trend during the most photochemically active months. In fact, a strong correlation between temperature and ozone during the warm season (May–September) in North America has already been shown by Chan (2009). It is therefore, important that the temperature effects be removed in the ozone variations in the summer, but not necessarily in the other seasons. It is important to note, however, that the correlation between observed ozone and local temperature during the warm season implies that the observed ozone must be affected by local/regional influences, even at these remote non-urban sites.

The results of the long-term trend analyses are not straightforward because the regions and the direction of the trends vary from season to season. The major results can be summarized as follows:

– In the Pacific coastal regions of southwestern British Columbia (Canada) and California (US), the decadal trends increased in all seasons except in the fall (SON)

in California. The trends were statistically significant in British Columbia in all seasons except in the fall, but were not significant in California in any of the seasons.

- In the Atlantic coastal zone, (encompassing southern New Brunswick and southern Nova Scotia in Canada and northeast Maine in the US), the trends were positive (but significantly so only in the spring), except in the winter when the trend was negative (but not significant). Hence, the only significant trend detected was an upward trend in the spring.

- The eastern part of Canada and the US (i.e., east of Lake Superior in Canada and east of the Mississippi River in the US) showed negative trends in all regions in all seasons, with three exceptions: (1) insignificant positive trends in Atlantic Canada/northeast Maine in the summer, fall and winter (discussed above), (2) a significant positive trend in winter (DJF) at sites in the US Midwest (Ohio, Indiana and Illinois), and (3) significant positive trends at all sites in Quebec (Canada) and one site in Vermont (US) during the summertime.

- At all sites in central/western Canada and the US, the trends tended to be negative in the spring and fall but positive in the summer and winter. The density of the sites in the central and western regions is very low which means that the regional representativeness of the data was considerably lower than for the regions in the east.

Although the individual regional *baseline* trends are difficult to interpret, collectively they exhibit similar tendencies over large areas of North America. For example, the Pacific and Atlantic coastal regions of Canada and the US generally exhibit positive trends. This is consistent with previous studies at remote and/or free troposphere sites that have documented increasing trends in overall mixing ratios, particularly in the winter and spring months, over the last two decades (Jaffe et al., 2003, 2007; Lelieveld et al., 2004; Jonson et al., 2006; Oltmans et al., 2006; Derwent et al., 2007; Tanimoto et al., 2009; Parrish et al., 2009; Cooper et al., 2010). Alternatively, the continental regions of central/western Canada and the US (except PC2, PC3 and PC4) tend to exhibit negative trends in the spring and fall and positive trends in the summer and winter.

A number of mechanisms leading to the increase in *baseline* levels have been suggested in the literature. Stohl et al. (2002), Cooper et al. (2005) and Owen et al. (2006) have shown that ground-level ozone can be lifted above the PBL where it can travel to other countries and continents in the northern mid-latitudes, thereby contributing to the *baseline* levels and trends of the other countries. Consistent with this, Cooper et al. (2010) have shown that, in western North America during the springtime, the rate of increase of the ozone mixing ratio in the free troposphere is greatest when the measurements are more heavily influenced by direct transport from Asia. For Europe, Ordóñez et al. (2007) present evidence to suggest, at least at high altitudes (3000–3500 m a.s.l.), that the positive trends in *baseline* ozone in winter-spring during the 1990s were likely due to higher levels of lower stratospheric ozone induced by the recovery of the ozone layer. This differs from western North America where Cooper et al. (2010) saw no evidence of changes in ozone levels in the lower stratosphere or changes in the frequency of stratospheric intrusions into the troposphere within their study region. Model studies by Li et al. (2002) and Derwent et al. (2004) indicate that increases in Asian precursor emissions alone do not explain the significant upward trends observed in tropospheric *baseline* ozone in Europe. As interesting as these studies are, they point to the need for continued research into the physical and chemical mechanisms responsible for the consistent increases in *baseline* ozone.

In contrast to the foregoing low (precursor) emission regions, the regions in the high NO_x and non-methane hydrocarbon (NMHC) emission areas of eastern Canada and the eastern US (viz., PC2, PC3 and PC4 in the MAM/JJA/SON, and PC2 and PC3 in the DJF maps of Fig. 7a and b) show consistently negative *baseline* and *most polluted* trends in all seasons, with the steepest trends occurring in the summer (with the one exception of PC2 (southeastern US) in DJF where the *most polluted* trend is positive – see Fig. 7b). In the US, the predominantly negative trends are consistent with the major decreases in NO_x emissions in those regions throughout the 2000 to 2007 time period (Canada–United States, 2008), and especially during the ozone season of May through September when emission reductions were highest. This relationship once again implies that these three regions are not continentally representative but, rather, are affected by within-region emissions. Additionally, the weaker negative trends (or in one case, positive trends) seen in these regions in the winter compared to other seasons are due to the reductions of NO_x emissions over the years, thereby resulting in less NO being available to destroy ozone outside of urban areas.

4.6 Diurnal variations of *baseline* mixing ratios

As a further diagnostic tool for understanding the nature of *baseline* ozone, seasonal-mean diurnal cycles of the sites in the 14 PCA-derived regions were determined by calculating a least-squared fit 24-h cycle to the 10-year data set of *hourly baseline* mixing ratios. Similar to Fig 5a and 5b, the individual panels are joined by lines to the regionally representative sites for the PCA/JJA groupings. Figures 8a and 8b show the seasonal-average diurnal cycles associated with the *baseline* and *most polluted* air clusters, respectively, for all of the PCA-derived regions. Diurnal variations that peak in the afternoon are influenced by the combined effects of vertical entrainment of air from aloft by the growing convective PBL, the inflow of ozone due to transport from outside the

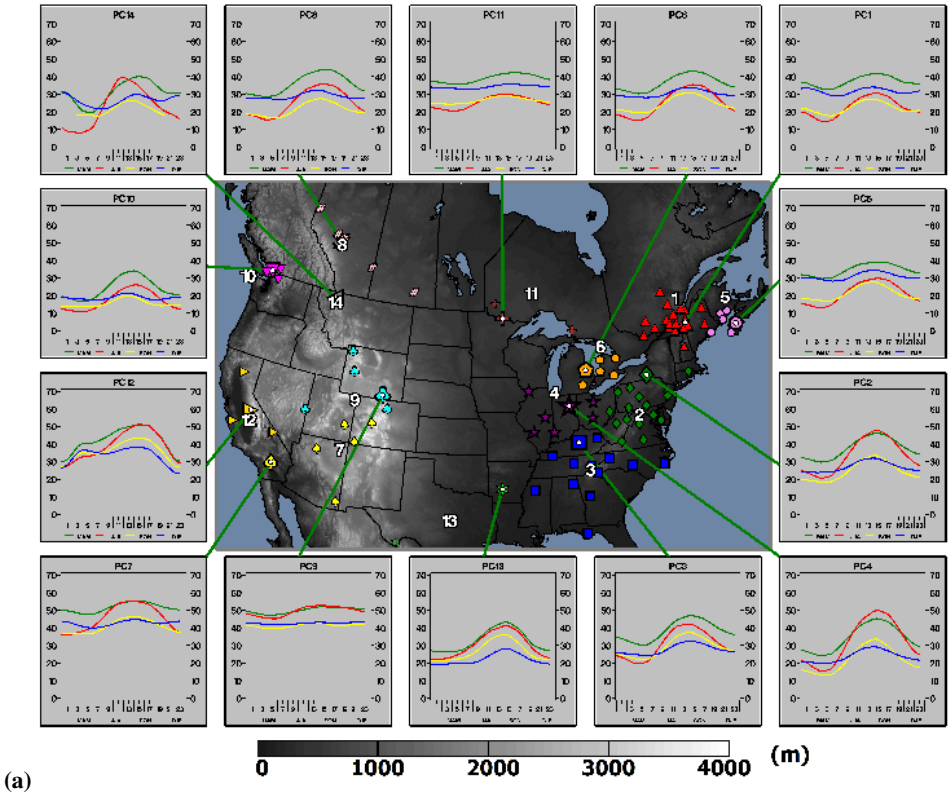

(a)

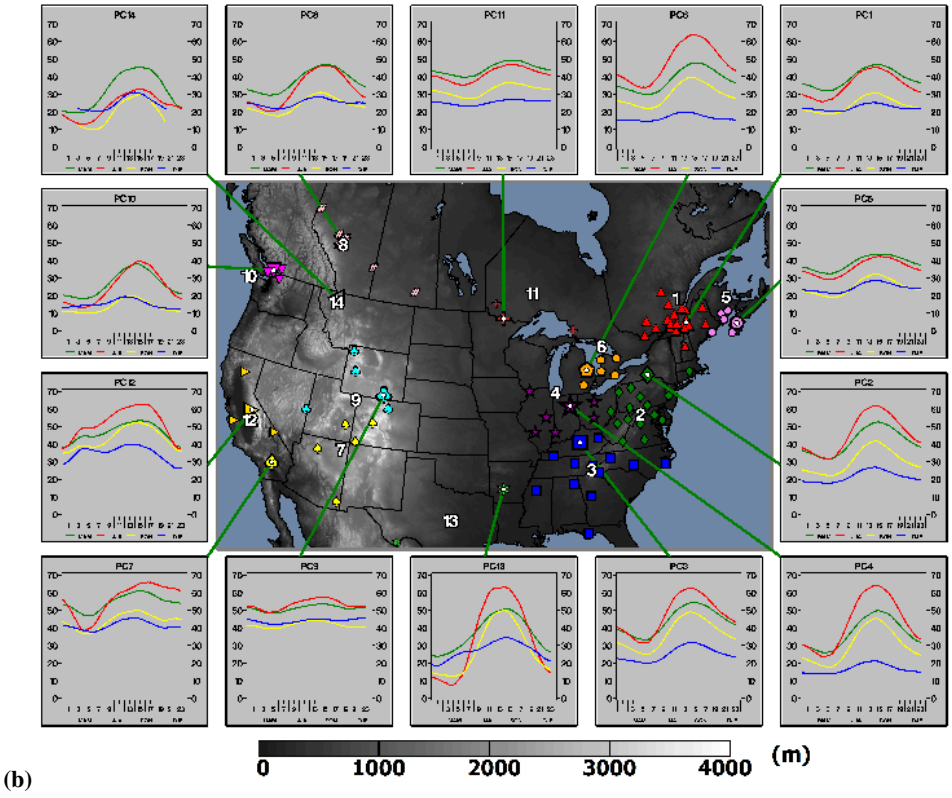

(b)

Fig. 8. (a): Seasonally averaged ozone diurnal variations associated with the *baseline* air trajectory clusters grouped by rotated PCA for JJA. **(b)**: Seasonally averaged ozone diurnal variations associated with the *most polluted* air trajectory clusters grouped by rotated PCA for JJA. Vertical axes represent ozone mixing ratios (ppb) and the tickmarks on the horizontal axes represent the start of each hour in local standard time (LST).

location, and in-situ photochemical production. Nighttime and early morning decreases in mixing ratios are expected to be related more to surface destruction than chemical scavenging because of the non-urban nature of the sites (i.e., distant from major NO_x sources) (Singh et al., 1978). In this study, additional insights are gained from the large number of non-urban sites affected by minimal-to-high regional anthropogenic NO_x and NMHC emission sources, and low-to-high elevation areas in Canada and the US.

In general, the peaks of the diurnal cycles associated with the *most polluted* air (Fig. 8b) are about 10 – 20 ppb higher than those of the *baseline* air (Fig. 8a) during the summer (JJA, red curves) and always lower during the winter (DJF, blue curves). This is not surprising given the strong influence of precursor emission sources in the *most polluted* air. The only exception to this is PC13, for which the nocturnal minimum associated with the *most polluted* air cluster is lower than that associated with the *baseline* air cluster, although the daytime maximum associated with the *most polluted* air cluster is higher than that associated with the *baseline* air cluster.

The diurnal cycles associated with the *most polluted* air are always of higher amplitude than those associated with the *baseline* air in the daytime during the summer (JJA). This suggests that additional amounts of inflow ozone are transported to the sites from upwind precursor sources, which dominates over the ozone that is vertically mixed down to the surface during the day and scavenged and/or surface deposited during the night. The absence of a strong diurnal cycle in the *baseline* cluster in some regions like the Continental Western US (e.g. PC9, which consists of high elevation sites) suggests that the trajectory selection strategy has, in those regions, most satisfactorily selected *baseline* ozone. This is because most high elevation measurement sites are expected to be exposed to air from the free troposphere more frequently than low elevation air that has been lifted vertically from lower elevations, thereby leading to smaller diurnal variations at the high elevation sites than at sites near sea level. This is indeed the case for PC9, the region that consists of the highest elevation sites. Here, mixing ratios decrease only minimally at night (Fig. 8a) which, in turn, suggests that depositional and chemical losses are minimal during this time of the day. Similarly, the lack of a strong daytime maximum suggests that daytime production of ozone from local precursors is minimal or, in other words, the long range transport of non-locally-produced ozone is the dominant source of ozone at these high elevation sites.

The magnitude and amplitude of the *baseline* ozone levels associated with the diurnal cycles (i.e., the highest and lowest values on the seasonal mean curves) are visible in Fig. 8a. They show that the Eastern US regions (PC2, PC3 and PC4), which are known for high precursor emissions, have very high mean diurnal peaks – up to 50 ppb. The high elevation regions of the Western US (PC7 and PC9) also have high levels (up to 55 ppb) but the diurnal cycles are of lower amplitude than in the Eastern US. Of all of the regions, the lowest levels of diurnal cycles occur in the Pacific coastal zone near Seattle, USA and Vancouver, Canada where the peak mixing ratio reaches 35 ppb.

5 Summary and conclusions

This study provides a comprehensive analysis of decadal, seasonal and diurnal temporal variations of *baseline* ozone in different regions of Canada and the US for the period 1997 to 2006. *Baseline* ozone mixing ratios for North America were estimated from measurements taken at 97 non-urban sites covering most of the populated areas of Canada and the US from 24° N to 56° N and 65° W to 123° W (ranging from 2 to 3178 m a.s.l.). The results indicate that, as one would expect, a single *baseline* ozone level cannot be defined for all of North America. Rather, *baseline* ozone, as defined here, varies geographically and seasonally. This conclusion is largely consistent with prior studies in which different methods were used to investigate *baseline* ozone variability (Lefohn et al., 2001; Fiore et al., 2003). However, this study extends beyond the prior work. As previously published by Parrish et al. (2009) and Jaffe et al. (2007), it finds that, at sites in coastal regions (coastal areas of the Pacific and Atlantic Oceans), *baseline* levels are predominantly influenced by flow off the oceans. In continental areas, *baseline* levels are shown to be predominantly associated with flows traveling over low precursor emission areas originating in high altitudes. As expected from the literature, it also finds that the seasonal *baseline* ozone variations in those regions located away from major precursor emission sources (mainly in Canada) were characterized by a single ozone maximum in the springtime (Fig. 5a) with no evidence of a secondary summertime maximum induced by photochemical production within the region.

Ten-year annual and seasonal average *baseline* mixing ratios are estimated for seven regions of Canada and the US in Table 1. Annual average mixing ratios vary from a low of 19±10 ppb in Coastal Western Canada (in the vicinity of Vancouver, British Columbia) to a high of 46±7 ppb in the Continental Western US (high elevation sites). Continental Eastern Canada (i.e., PC1, PC6, and PC11), which is known to have few anthropogenic precursor emission sources to the north of the measurement sites, has a lower summertime *baseline* level (24±8 ppb) than the Continental Eastern US (PC2, PC3 and PC4) where large anthropogenic precursor emission sources exist (32±12 ppb). The opposite is true for the winter season when Continental Eastern Canada has a *baseline* seasonal average of 32±5 ppb compared to 27±7 ppb in the Continental Eastern US. In spite of this, the annual average *baseline* mixing ratios of the two regions are quite similar at 30±9 and 30±10 ppb, respectively, as the two seasonal differences cancel out. This indicates that *baseline* levels in Continental Eastern Canada are minimally affected by within-region precursor emissions in the summer and the

winter (i.e., minimal within-region photochemical production in the summer and no NO scavenging in the winter). The opposite is true for the Continental Eastern US where within-region precursor emissions have a strong effect on the *baseline* levels through higher photochemical production in the summer and some NO scavenging in the winter.

The decadal trends of *baseline* ozone vary from region to region and season to season, with some of the trends being statistically significant and others not (based on our GLMM trend model). In spite of this variability, the trends exhibit consistent behavior over large areas of North America. Specifically, consistent with previous studies, the Pacific and Atlantic coastal regions exhibit positive trends, the continental areas of central/western North America exhibit negative trends in the spring/fall and positive trends in the summer/winter, and the high precursor emission areas of eastern Canada and the Eastern US consistently exhibit negative trends in all seasons except winter (in both the *baseline* and *most polluted* clusters). As mentioned earlier, the negative trends in the high emission areas were concomitant with major decreases in NO_x emissions in those regions. As an illustration, in MAM, *baseline* ozone increased by 0.28 ppb/a in Coastal Western Canada (PC10) but decreased by 0.59 ppb/a in the high precursor emission area of the Eastern US (PC2). From the literature, positive trends in *baseline* ozone (ranging from 0.3 to 1 ppb/a) appear to be a large-scale phenomenon in the northern hemisphere, having been reported in Greenland (Helmig et al., 2007), Switzerland (Brönnimann et al., 2002), the North Atlantic (Lelieveld et al., 2004), Ireland (Simmonds et al., 2004; Derwent et al., 2007), continental Europe (EMEP, 2005), Japan (Tanimoto, 2009), China (Wang et al., 2009). This suggests that the negative *baseline* trends in the high precursor emission areas of the Eastern Canada and Eastern US are the net result of an increasing trend in *baseline* air coupled with a decreasing trend in within-region air, the latter being attributable to major precursor emission reductions. This implies that the decreasing trends seen in the *baseline* and *most polluted* air of the high precursor regions would have, in fact, decreased even more if the *baseline* trend had not been positive.

The foregoing discussion suggests that the apparent hemispheric increase in *baseline* ozone has had two major impacts: (1) it has directly increased the ambient ozone levels in the low precursor emission areas of North America and (2) it has reduced, to some degree, the efficacy of precursor emission control efforts in the high precursor emission areas of North America, namely, Eastern Canada and the Eastern US. In the future, if *baseline* ozone levels continue to rise in the northern hemisphere while within-region ozone levels continue to decrease or level off in the high emission areas (due to the leveling off of emission controls), then the relative contribution of *baseline* ozone to overall ambient ozone levels would be expected to increase.

Acknowledgements. Thanks are due to Pierrette Blanchard (Environment Canada/Science and Technology Branch, Toronto, Canada) for scientific advice, Michael Shaw (Environment Canada/Science and Technology Branch, Toronto, Canada) for many SAS/GRAPH software's macros and subroutines, and Jacinthe Racine and the Air Quality Modelling and Application Section (Environment Canada/Science and Technology Branch, Montreal, Canada) for performing numerous trajectory calculations. The authors are very grateful for the insightful comments provided by the anonymous reviewers.

Edited by: U. Pöschl

References

Altshuller, A. P.: Estimation of the natural background of ozone present at surface rural locations, J. Air Pollut. Control Assoc., 37, 1409–1417, 1987.

Altshuller, A. P. and Lefohn, A. S.: Background ozone in the planetary boundary layer over the United States, J. Air Waste Manage. Assoc., 46, 134–141, 1996.

Brönnimann, S., Buchmann, B., and Wanner, H.: Trends in near surface ozone concentrations in Switzerland: The 1990s, Atmos. Environ., 36, 2841–2852, doi:10.1016/S1352-2310(02)00145-0, 2002.

Brook, J. R., Strawbridge, K., Snyder, B. J., et al.: Towards an understanding of the fine particle variations in the LFV: integration of chemical, physical and meteorological observations, Atmo. Environ., Volume 38, Issue 34, The Pacific 2001 Air Quality Study, November 2004, 5775–5788, ISSN 1352-2310, doi:10.1016/j.atmosenv.2004.01.056, 2004.

Burnett, R. T., Brook, J. B., Yung, W. T., Dales, R. E., and Krewski, D.: Association between Ozone and Hospitalization for Respiratory Diseases in 16 Canadian Cities, Environ. Res., 72, 1, 1996, 24–31, ISSN 0013-9351, doi:10.1006/enrs.1996.3685, 1996.

Canada, Regulatory Framework for Air Emissions, Report on Canada's New Government announces targets to tackle climate change and reduce air pollution, available online at: http://www.ecoaction.gc.ca/, 2007.

Canada–United States, Canada-United States Air Quality Agreement-Progress Report 2008. available online at: http://www.ec.gc.ca/Publications/default.asp?lang=En\&xml=D8E5913D-0A85-4BE4-AD67-B627D0C0FE87, 2008.

Center for International Earth Science Information Network (CIESIN): Gridded Population of the World: Future Estimates, Socioeconomic Data and Applications Center (SEDAC), Columbia University, Palisades, NY, USA, available online at: http://sedac.ciesin.columbia.edu/gpw, 2005.

Chan, E.: Regional ground-level ozone trends in the context of meteorological influences across Canada and the eastern United States from 1997 to 2006, J. Geophys. Res., 114, D05301, doi:10.1029/2008JD010090, 2009.

Cleveland, W. S., Devlin, S. J., and Grosse, E.: Regression By Local Fitting, J. Econometr., 37, 87–114, 1988.

Cooper, O. R., Stohl, A., Eckhardt, S., et al.: A springtime comparison of tropospheric ozone and transport pathways on the east and west coasts of the United States, J. Geophys. Res., 110, D05S90, doi:10.1029/2004JD005183, 2005.

Cooper, O. R., Parrish, D. D., Stohl, A. et al., Increasing springtime ozone mixing ratios in the free troposphere over western North America, Nature, 463, 344-348, doi:10.1038/nature08708, 2010.

Côté, J., Desmarais, J.-G., Gravel, S., Méthot, A., Patoine, A., Roch, M., and Staniforth, A.: The Operational CMC/MRB global environmental multiscale (GEM) model, available online at: http://www.msc-smc.ec.gc.ca/cmc_library/index_e.html – select "Forecast", then sign in, 2007.

D'Amours, R., and Pagé, P.: Atmospheric Transport Models for Environmental Emergencies – The Trajectory Model, Canadian Meteorological Centre, 2121 Trans-Canada Highway, Dorval, Quebec H9P 1J3, Canada, available online at http://collaboration.cmc.ec.gc.ca/cmc/cmoi/product_guide/docs/lib/model-eco_urgences_e.pdf, 2001.

Daniesen, E. F. and Mohnen, V. A.: Project Dustorm report: ozone transport, in situ measurements, and meteorological analyses of tropopause folding, J. Geophys. Res., 82, 5867–5877, 1977.

Derwent, R. G., Jenkin, M. E., Saunders S. M., et al.: Photochemical ozone formation in north west Europe and its control, Atmo. Environ., 37(14), 1983–1991, ISSN 1352–2310, doi:10.1016/S1352-2310(03)00031-1, 2003.

Derwent, R. G., Stevenson, D. S., Collins, W. J., and Johnson, C. E.: Intercontinental transport and the origins of the ozone observed at surface sites in Europe, Atmos. Environ., 38, 1891–1901, 2004.

Derwent, R. G., Simmonds, P. G., Manning, A. J., and Spain, T. G.: Trends over a 20-year period from 1987 to 2007 in surface ozone at the atmospheric research station, Mace Head, Ireland, Atmos. Environ., 41(39), 9091–9098, 2007.

Dorling, S. R., Davies, T. D., and Pierce, C. E.: Cluster analysis: A technique for estimating the synoptic meteorological controls on air and precipitation chemistry – Method and applications, Atmos. Environ., 26A, 2575–2581, 1992.

Eder, B. K., Davis, J. M., and Bloomfield, P.: A Characterization of the Spatiotemporal Variation of Non-Urban Ozone in the Eastern United States, Atmos. Environ., 27A, 2645–2668, 1993.

Ehhalt, D. H.: Gas phase chemistry of the troposphere, Topic. Phys. Chem., 6, 21–109, 1999.

EMEP: The development of European surface ozone. Implications for a revised abatement policy, EMEP/CCC-Rep., 1/2005, Norw. Inst. for Air Res., Oslo, Norway, available online at http://www.nilu.no/projects/CCC/reports.html), 2005.

Fiore, A. M., Jacob, D. J., Bey, I., Yantosca, R. M., Field, B. D., Fusco, A. C., and Wilkinson, J. G.: Background ozone over the United States in summer: Origin, trend, and contribution to pollution episodes, J. Geophys. Res., 107(D15), 11-1–11-25, doi:10.1029/2001JD000982, 2002.

Fiore, A., Jacob, D. J., Liu, H., Yantosca, R. M., Fairlie, T. D., and Li, Q.: Variability in surface ozone background over the United States: Implications for air quality policy, J. Geophys. Res., 108(D24), 4787, doi:10.1029/2003JD003855, 2003.

Fiore, A. M., West, J. J., Horowitz, L. W., Naik, V., and Schwarzkopf, M. D.: Characterizing the tropospheric ozone response to methane emission controls and the benefits to climate and air quality, J. Geophys. Res., 113, D08307, doi:10.1029/2007JD009162, 2008.

Gauss, M., Myhre, G., Isaksen, I. S. A., et al.: Radiative forcing since preindustrial times due to ozone change in the troposphere and the lower stratosphere, Atmos. Chem. Phys., 6, 575–599, doi:10.5194/acp-6-575-2006, 2006.

Goldstein, A. H., Millet, D. B., McKay, M., et al.: Impact of Asian emissions on observations at Trinidad Head, California, during ITCT 2K2, J. Geophys. Res., 109, D23S17, doi:10.1029/2003JD004406, 2004.

Hayden, K. L., Anlauf, K. G., Li, S.-M., et al.: Characterization of gaseous nitrogen oxides in the Lower Fraser Valley during Pacific 2001, Atmo. Environ., Volume 38, Issue 34, The Pacific 2001 Air Quality Study, November 2004, 5811–5823, ISSN 1352-2310, doi:10.1016/j.atmosenv.2003.12.048, 2004.

Hocking, W. K., Carey-Smith, T, Tarasick, D. W., et al.: Detection of stratospheric ozone intrusions by wind profiler radars, Nature, 450, 281–284, doi:10.1038/nature06312, 2007.

Intergovernmental Panel on Climate Change (IPCC), Climate Change 2001: The Scientific Basis – Contribution of Working Group I to the Third Assessment Report of the Intergovernmental Panel on Climate Change, edited by: Houghton, J. T., Ding, Y., Griggs, D. J., et al., Cambridge Univ. Press, NY, USA, 2001.

Intergovernmental Panel on Climate Change (IPCC), Climate Change 2007: The Physical Science Basis, in: Contribution of Working Group I to the Fourth Assessment Report of the Intergovernmental Panel on Climate Change, edited by: Solomon, S., Qin, D., Manning, M., et al., Cambridge University Press, Cambridge, UK and New York, NY, USA, 2007.

Jaffe, D., Price, H., Parrish, D., Goldstein, A., and Harris, J.: Increasing background ozone during spring on the west coast of North America, Geophys. Res. Lett., 30(12), 1613, doi:10.1029/2003GL017024, 2003.

Jaffe, D. and Ray, J.: Increase in surface ozone at rural sites in the western US, Atmos. Env., 41, 5452–5463, ISSN 1352-2310, doi:10.1016/j.atmosenv.2007.02.034, 2007.

Jaffe, D., Chand, D., Hafner, W., Westerling, A. and Spracklen D.: Influence of fires on O_3 concentrations in the western U.S., Environ. Sci. Technol., 42(16), 5885–5891, doi:10.1021/es800084k, 2008.

Jenkin, M. E.: Trends in ozone concentration distributions in the UK since 1990: Local, regional and global influences, Atmo. Environ., 42(21), 5434–5445, ISSN 1352-2310, doi:0.1016/j.atmosenv.2008.02.036, 2008.

Johnson, C. E., Collins, W. J., Stevenson, D. S., and Derwent, R. G.: Relative roles of climate and emissions changes on future tropospheric oxidant concentrations, J. Geophys. Res., 104(D15), 18631–18645, 1999.

Jonson, J. E., Simpson, D., Fagerli, H., and Solberg, S.: Can we explain the trends in European ozone levels?, Atmos. Chem. Phys., 6, 51–66, doi:10.5194/acp-6-51-2006, 2006.

Karlsson, P. E., Pleijel, H., Danielsson, H., Karlsson, G. P., Piikki, K., et al.: Evidence for Impacts of Near-ambient Ozone Concentrations on Vegetation in Southern Sweden, AMBIO: A Journal of the Human Environment, 38(8), 425–432, 2009.

Lefohn, A. S., Oltmans, S. J., Dann, T., and Singh, H. B.: Present-day variability of background ozone in the lower troposphere, J. Geophys. Res., 106(D9), 9945–9958, 2001.

Lelieveld, J., Aardenne, J. van, Fischer, H., de Reus, M., Williams, J., and Winkler, P.: Increasing ozone over the Atlantic Ocean, Science, 304, 1483–1487, 2004.

Li, Q., Jacob, D. J., Bey, I., et al.: Transatlantic transport of pollution and its effects on surface ozone in Europe and North America, J. Geophys. Res., 107(D13), 4166,

doi:10.1029/2001JD001422, 2002.

Lin, C. Y., Jacob, D. J., Munger, J. W., and Fiore, A. M.: Increasing background ozone in surface air over the United States, Geophys. Res. Lett., 27(21), 3465–3468, 2000.

Littell, R. C., Milliken, G. A., and Stroup, W. W.: SAS System for Mixed Models, 2nd ed., SAS Inst., Cary, NC, USA, 2006.

Logan, J. A.: Tropospheric ozone: seasonal behavior, trends, and anthropogenic influence, J. Geophys. Res. 90(D6), 10463–10482, 1985.

McLaren, R., Wojtal, P., Majonis, D., McCourt, J., Halla, J. D., and Brook, J.: NO_3 radical measurements in a polluted marine environment: links to ozone formation, Atmos. Chem. Phys., 10, 4187–4206, doi:10.5194/acp-10-4187-2010, 2010.

Monks, P. S.: A review of the observations and origins of the spring ozone maximum, Atmos. Environ., 34, 3545–3561, 2000.

Owen, R. C., Cooper, O. R., Stohl, A., and Honrath, R. E.: An analysis of the mechanisms of North American pollutant transport to the central North Atlantic lower free troposphere, J. Geophys. Res., 111, D23S58, doi:10.1029/2006JD007062, 2006.

Oltmans, S., Lefohn, A. S., Harris, J. M., et al.: Long-term changes in tropospheric ozone, Atmos. Environ., 40, 3156–3173, 2006.

Oltmans, S. J., Lefohn, A. S., Harris, J. M., and Shadwick D.: Background ozone levels of air entering the west coast of the U.S. and assessment of longer-term changes, Atmos. Environ. 42:6020–6038, 2008.

Ordóñez, C., Brunner, D., Staehelin, J., et al.: Strong influence of lowermost stratospheric ozone on lower tropospheric background ozone changes over Europe, Geophys. Res. Lett., 34, L07805, doi:10.1029/2006GL029113, 2007.

Parrish, D. D., Millet, D. B., and Goldstein, A. H.: Increasing ozone in marine boundary layer inflow at the west coasts of North America and Europe, Atmos. Chem. Phys., 9, 1303–1323, doi:10.5194/acp-9-1303-2009, 2009.

Penkett, S. A. and Brice, K. A.: The spring maximun in photooxidants in the Northern Hemisphere troposphere, Nature, 319, 655–657, 1986.

Prinn, R. G.: The cleansing capacity of the atmosphere, Ann. Rev. Environ. Resour., 28, 29–57, doi:10.1146/annurev.energy.28.011503.163425, 2003.

Ramaswamy, V., Boucher, Haigh, J., et al.: Chapter 6. Radiative Forcing of Climate Change, Climate Change 2001: The Scientific Basis, edited by: Joos, F., Srinivasan, J., Cambridge Univ. Press, New York, USA, 2001.

The Royal Society, Ground-level ozone in the 21^{st} Century: Future trends, impacts and policy implications, Science Policy Report 15/08, 2008.

SAS/STAT User's Guide, Version 6, 4th Edition, Vol. 2, Cary, NC, SAS Institute Inc., 1990.

SAS/STAT Software: The GLIMMIX Procedure, User's Guide, Cary, NC, SAS Institute Inc., 2006.

Simmonds, P. G., Seuring, S., Nickless, G., and Derwent, R. G.: Segregation and interpretation of ozone and carbon monoxide measurements by air mass origin at the TOR station Mace Head, Ireland from 1987 to 1995, J. Atmos. Chem., 28, 45–49, 1997.

Simmonds, P. G., Derwent, R. G., Manning, A. J., and Spain, G.: Significant growth in surface ozone at Mace Head, Ireland, 1987–2003, Atmos. Environ., 38, 4769–4778, doi:10.1016/j.atmosenv.2004.04.036, 2004.

Singh, H. B., Ludwig, F. L., and Johnson, W. B.: Tropospheric ozone: concentrations and variabilities in clean remote atmospheres. Atmos. Environ., 12, 2185–2196, 1978.

Stevenson, D. S., Dentener, F. J., Schultz, M. G., et al.: Multimodel ensemble simulations of present-day and near-future tropospheric ozone, J. Geophys. Res., 111, D08301, doi:10.1029/2005JD006338, 2006.

Stohl, A., Eckhardt, S., Forster, C., James, P., and Spichtinger, N.: On the pathways and timescales of intercontinental air pollution transport, J. Geophys. Res., 107(D23), 4684, doi:10.1029/2001JD001396, 2002.

Task Force on Hemispheric Transport of Air Pollution (TF HTAP): Hemispheric transport of air pollution 2010 assessment report, edited by: Keating, T. J. and Zuber, A., draft, available online at: http://www.htap.org, 2010.

Tanimoto, H.: Increase in springtime tropospheric ozone at a mountainous site in Japan for the period 1998-2006, Atmo. Environ., Volume 43, Issue 6, February 2009, 1358–1363, ISSN 1352-2310, doi:10.1016/j.atmosenv.2008.12.006, 2009.

US EPA: Air quality criteria for ozone and related photochemical oxidants (Final), Vol. I, II, and III, EPA 600/R-05/004aF-cF, 2006.

US EPA: NO_x Budget Program 2006 Progress Report, available online at: http://www.epa.gov/airmarkt/progress/nbp06.html, 2007.

US EPA: National Ambient Air Quality Standards for Ozone, Proposed Rules, available online at: http://www.epa.gov/air/ozonepollution/fr/20100119.pdf, 2010.

Viezee, W., Johnson, W. B., and Singh, H. B.: Stratospheric ozone in the lower troposphere-II. Assesment of downward flux and ground-level impact, Atmos. Environ., 17, 1979–1993, 1983.

Vingarzan, R.: A review of surface ozone background levels and trends, Atmos. Environ. 38, 3431–3442, 2004.

Wang, Y., Shim, C., Blake, N., et al.: Intercontinental transport of pollution manifested in the variability and seasonal trend of springtime O_3 at northern middle and high latitudes, J. Geophys. Res., 108(D21), 4683, doi:10.1029/2003JD003592., 2003.

Wang, H., Jacob, D. J., Le Sager, P., et al.: Surface ozone background in the United States: Canadian and Mexican pollution influences, Atmos. Environ., 43(6), 1310–1319, doi:10.1016/j.atmosenv.2008.11.036, 2009.

Wang, T., Wei, X. L., Ding, A. J., et al.: Increasing surface ozone concentrations in the background atmosphere of Southern China, 1994–2007, Atmos. Chem. Phys., 9, 6217–6227, doi:10.5194/acp-9-6217-2009, 2009.

West, J. J., Fiore, A. M., Naik, V., Horowitz, L. W., Schwarzkopf, M. D., and Mauzerall, D. L.: Ozone air quality and radiative forcing consequences of changes in ozone precursor emissions, Geophys. Res. Lett., 34, L06806, doi:10.1029/2006GL029173, 2007.

Wild, O.: Modelling the global tropospheric ozone budget: exploring the variability in current models, Atmos. Chem. Phys., 7, 2643–2660, doi:10.5194/acp-7-2643-2007, 2007.

Zeng, G., Pyle, J. A., and Young, P. J.: Impact of climate change on tropospheric ozone and its global budgets, Atmos. Chem. Phys., 8, 369–387, doi:10.5194/acp-8-369-2008, 2008.